

Measurements and modeling of soil water distribution around landmines in natural soil

Henk A. Lensen^a, Piet B.W. Schwering^a, Garciela Rodríguez Marín^b, Jan M.H. Hendrickx^b

^aTNO Physics and Electronics Laboratory, P.O. Box 96864, NL-2509 JG The Hague, Netherlands, Lensen@fel.tno.nl

^bNew Mexico Tech, 801 LeRoy Place, Socorro NM 87801, USA, hendrick@nmt.edu

ABSTRACT

Soil water content, dielectric constant, electrical conductivity, thermal conductivity and heat capacity affect the performance of many sensors (e.g. GPR, TIR) and therefore the detection of landmines. The most important of these is water content since it directly influences the other properties. We measure soil water distribution around an antitank and an antipersonnel mine buried in a sand soil under varying moisture levels. After a period of two days with 38 mm precipitation the water content below the AP-mine increased from 0.07 to 0.12 [m³/m³]. The water content above and below the AT-mine increased from 0.09 to 0.17 [m³/m³] and 0.09 to 0.13 [m³/m³], respectively. Below the AT-mine it was 0.02 to 0.04 [m³/m³] dryer than above the mine. The dielectric constant of the soil was estimated from the soil water content. After a dry period of two weeks the dielectric contrast between the AT-mine was approximately 2 [F/m]. After a period of 38 mm precipitation the contrast between AT-mine and background increased to 6 [F/m]. Differences in soil water distribution around the AT-mine caused a maximum dielectric contrast 4.5 [F/m] between background and mine. This effect was less apparent around the AP-mine (1.3 [F/m]). Differences in measured and simulated soil water distribution around an AT-mine urge for further investigation.

Keywords: Mine detection, soil water distribution, modeling, antitank mine, antipersonnel mine, test facility, dielectric constant.

1. INTRODUCTION

Soil water content, dielectric constant, electrical conductivity, thermal conductivity and heat capacity affect the performance of many sensors such as ground penetrating radar (GPR) and thermal infrared imager (TIR). The most important of these is water content since it directly influences the other properties. Knowledge of water distribution in soils and the effect of mines on this distribution can therefore help to predict performance of these sensors, or a combination of these sensors in a sensor fused system. Moreover, the performance can be improved by optimizing the soil water distribution for a certain sensor or a combination of sensors by for example wetting¹ or drying². Knowledge of the soil water distribution in soils and the effect of mines on this distribution can therefore improve the detection of landmines.

The goal of this paper is to gain more inside into the soil water distribution in natural soil and the effect of buried mines on this distribution.

For this reason an antipersonnel (AP) and antitank (AT) mine were buried in a test lane with a sand soil. In order to measure the soil water distribution in the soil water content reflectometers (WCR) were placed above and below the mines and at four reference depths. During a 6-week field trial (January 26th – March 9th 2001) the water content was recorded together with meteorological data such as precipitation. The mines and WCRs had been installed 1-2 month prior to the field trial. The dielectric contrast between the buried landmines and the background soil was estimated using an empirical relation between soil water content and dielectric constant. Next the consequences for the detection of the landmines with a GPR-system was considered.

A model was used to predict the soil water distribution around an AT-mine in a soil with the same characteristics as the sand soil of the field trial. Precipitation and evaporation values of 1991 of a location at approximately 100-km distance from the field location were used for the model simulation. Next the results of the simulation and field trial were examined to give a first impression of the validation of the model.

The set up of the field experiments and model simulation are described in section 2. In sections 3 the results of the experiments and modeling effort are discussed. Finally in section 4 conclusions are drawn.

2. SOIL WATER DISTRIBUTION AROUND LANDMINES

In this section both the field experiments and model simulation are described. First the test facility for the field experiments is discussed briefly. The results of the field experiments are discussed in the next section. These results were based on measurements carried out in a test lane with sand soil. In this soil a surrogate AP- and AT-mine were buried together with

soil moisture sensors. In section 2.1.2 the setup for the field experiment is described. Before the soil moisture sensors were installed a calibration has been carried out in the laboratory for the different soils of the test facility. In section 2.1.3 calibration matters are discussed. Finally in the section the model and simulation parameters are discussed briefly (§ 2.2).

2.1 Measurements of soil water distribution around landmines

2.1.1 Test facility at TNO

The field experiments were carried out at the test facility for landmine detection systems at TNO³. This test facility is situated on the proving ground 'Waalsdorp' near TNO Physics and Electronics Laboratory (TNO-FEL). It entails six test lanes filled with different soil types, surrogate mines and mine-like objects. All of the separate test lanes are covered by a moveable sensor platform.

The test lanes each are 10 m long, 3 m wide and 1.5 m deep. Four lanes are filled with a native soil with original structure and texture. These soils include sand, clay, peat and a ferromagnetic soil. A fifth lane is filled with a sandy soil with forest remnants like roots and twigs. A sixth lane is filled with a sandy soil but also has a vegetation cover. The soils of the other lanes are bare.

An important parameter for the performance of the sensors is the soil water content, since it affects electromagnetic and thermal properties. Therefore this test facility has the opportunity to regulate soil water by controlling the groundwater level for each test lane separately. This opens to the possibility of testing and interpreting the performance of detection systems under different soil water conditions.

Two systems have been installed to measure temperature and soil water profiles of the different soils. In addition the temperature is recorded of several surrogate mines. These measurements are carried out in order to gain insight into the temperature and water distribution within the soils and around the buried mines, which is especially useful in case of modeling the thermal or electromagnetic soils and mines. A weather station has been placed to record parameters like precipitation, ambient temperature, short wave and long wave irradiance, relative humidity, wind speed and wind direction.

A set of test objects, representing anti-personnel mines, anti-tank mines, and false targets (stones, cans etc.) have been placed at various depths (0-30 cm) in the test lanes. The mines are made of various materials and have different shapes and sizes. Non-metal mines, mines with a casing made out of plastic, metal or another material are included. The test mines have signatures close to those of real mines. To simulate the explosives, the devices have been filled with a silicone rubber.

2.1.2 Experimental set up

The field experiments were carried out from January 26th - March 9th, 2001. For this purpose several test lanes of the test facility were equipped with WCR Water Content Reflectometers (WCR) of Campbell Scientific, Inc⁴. These WCR were placed above and below AP- and AT-mines buried at different depth in different soils. Also reference WCRs were placed at some distance from the mines, but at same depths. The WCRs and mines were buried at the end of 2000. Ambient and soil temperatures at different depth were recorded simultaneously.

The field experiments described in this paper focus on the test lane with sand and clay. In these two lanes an area has been reserved for the installation of an AT- and an AP-mine. The AT-mine is a surrogate Netherlands mine of type NR26, which is a low-metal mine with cylindrical shape. The diameter is 30.0 cm and a height of 11.5 cm. The surrogate mine consists of mainly silicon rubber (RTV 3110 produced by Dow Corning Europe, Brussels). The AP-mine is a surrogate US mine of type M14, which is a low-metal mine with cylindrical shape. The diameter is 5.6 cm and a height of 4.2 cm. The surrogate mine consists of mainly silicon rubber with a plastic casing.

Table 1 gives the properties of RTV3110 compared to other explosives (TNT, Composition B-3, Tetryl) used in mines. This table shows that RTV3110 is a good surrogate of TNT since both substances have the same dielectric constant. The surrogate mines are depicted in Figure 1.

Table 1. Properties of RTV3110 and some high explosives. The dielectric constant is measured at the frequency given in brackets.

Properties	RTV3110	TNT	Comp B-3	Tetryl
Density (g/cm ³)	1,17 ⁵	1,56 ⁷	1,7 ⁷	1,7 ⁷
Dielectric constant	2,90 ⁵ (1 MHz)	2,88 ⁶ (5 MHz)		
	2,89 ⁵ (1 GHz)		3,25 ⁶ (3 GHz)	3,10 ⁶ (35 GHz)

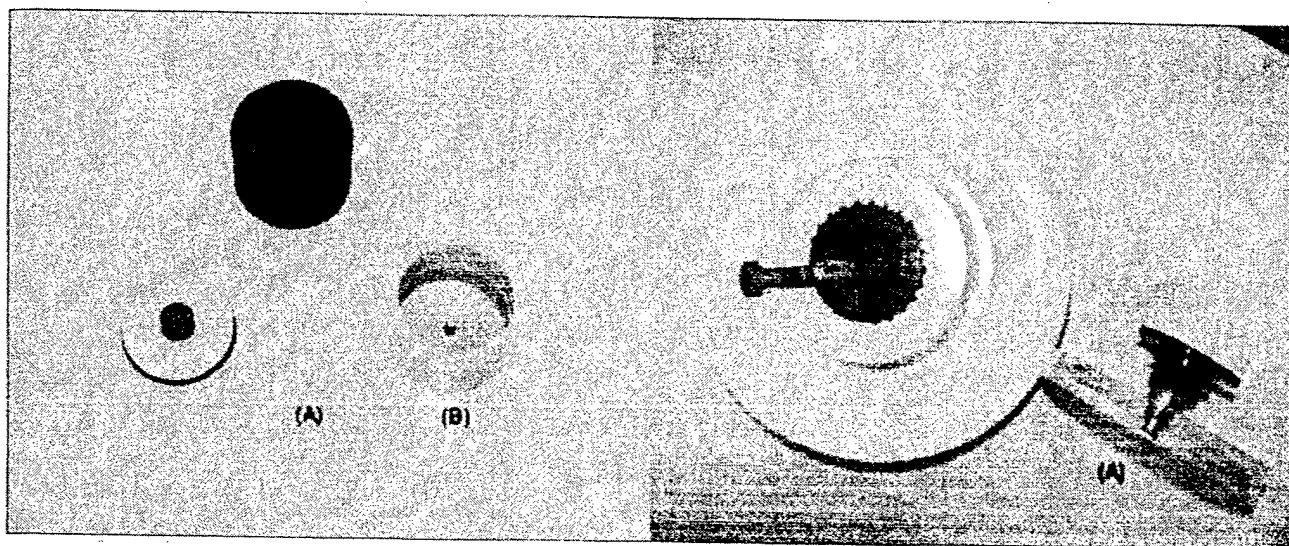


Figure 1. Surrogate M14 AP-mine (left) and NR26 AT-mine (right).

Figure 2 shows the instrumental set up for this experiment. The sand test lane has 8 WCRs. In each lane a WCR is placed just above (1 cm) and just below (1 cm) an AP- and an AT-mine. In the same area for each depth a reference WCR is installed. The AP-mines were buried at a depth of 10 cm (top) and the WCR above and below the mine and the references at depths 9 cm and 16 cm, respectively. The AT-mines were buried at a depth of 30 cm (top) and the WCR above and below the mine and the references at depths 29 cm and 44 cm, respectively.

The WCRs around the AP-mine are further referred to as 'AP low' for the one placed at a depth of 16 cm and 'AP high' for the one placed at a depth of 9 cm. The references WCR for the AP mines respectively, 'AP ref-low' and 'AP ref-high'. The same format is used for the WCRs placed left of the AT-mine (in Figure 1). When the WCRs are placed in for example sand the word 'sand' is added to the abbreviation (e.g. 'Sand AT ref-low' for the reference WCR at a depth of 44 cm).

The sets of high and low WCR are placed with a spatial separation of 40 cm. A Campbell AM-416 multiplexer and a CR10X datalogger were used to measure the soil water content and store it every 10 minutes. The measurements were carried out sequentially in order to prevent interference of the probes.

For the benefit of interpreting the measured data, ambient temperature and soil temperature profiles were measured and recorded. These recordings were done every 5 minutes.

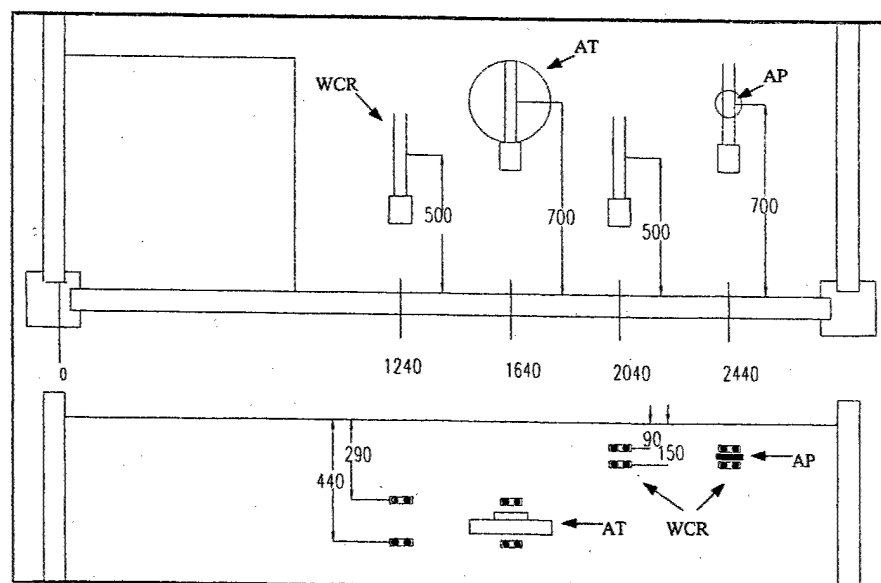


Figure 2. AP and AT-mine configuration with CS615 water content reflectometer (WCR) in test lane, viewed from the top (above) and aside (below). The dimensions are in millimetre and the drawing is not to scale

2.1.2 Calibration of WCR

The WCR water content reflectometer provides a measure of the volumetric water content (θ_v) of a porous media. The water content information is derived from the effect of changing dielectric constant on the electromagnetic waves propagating along a wave-guide. The propagation is also affected by the electrical conductivity. The amount of organic matter and clay in a soil can also alter the response of the dielectric-dependent methods to changes in water content. It is therefore suggested to calibrate the WCR for soils with a high electrical conductivity, high organic matter, high clay or high quartz content⁴.

In Table 2 the calibration curves are provided used in this study. For sand the calibration values reported by Campbell⁴ were used. For clay situated in the 'clay' test lane the calibration values acquired were quite different as expected. The calibration was done at 20°C with soil water contents varying from 0.16-0.46 (volume fraction, θ_v) for clay. Table 2 shows that the volumetric water content is largely overestimated for the clay soil when the calibration for sand is used.

Table 2. WCR calibration values at 20°C

Soil type	Calibration
Sand ⁴	$\theta_v = -0.187 + 0.037 * \tau + 0.335 * \tau^2$
Clay	$\theta_v = -1.018 + 1.729 * \tau - 0.505 * \tau^2$

With:

θ_v = volumetric water content [m^3/m^3];

τ = WCR output period [msec];

2.3 Simulation of soil water distribution around landmines

Soil water distributions around landmines have been modeled with the HYDRUS-2D simulation package⁵ of the U.S. Salinity Laboratory at Riverside, California. HYDRUS-2D is a Microsoft Windows based modeling environment for simulating two-dimensional water, heat, and solute movement and root water uptake in variably saturated soil. The flow equations are solved numerically using a Galerkin-type linear finite element scheme. The software includes a mesh generator and graphical user interface.

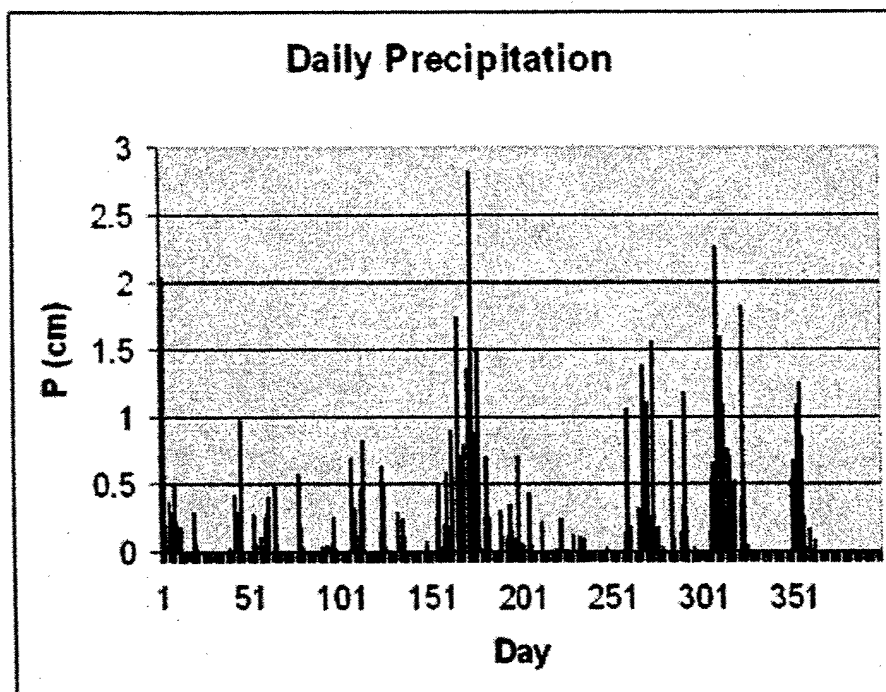


Figure 3. Daily values of precipitation in De Bilt, The Netherlands, during 1991.

For the landmine problem, we have followed earlier work by Das et al.⁹ and Hendrickx et al.¹⁰ and used a quasi three-dimensional region exhibiting radial symmetry about the vertical axis. Richards equation was solved to simulate unsaturated water flow in a soil cylinder with a radius of 2 m and depth of 2 m. The antitank mine was placed in the center of the cylinder with its top at a depth of 0.30 m. The antipersonnel mine was placed at the center of the cylinder with its top at a depth of 10

cm. A finite element mesh was generated by the mesh generator provided with the HYDRUS-2D program. Observation points were located approximately one centimeter above and one centimeter below the mine about 1 cm away from its center. The top boundary condition of the soil cylinder was determined by the atmospheric conditions. A constant ground water level at 150 cm below the soil surface was assigned to the bottom boundary. A no-flux boundary condition was imposed on two sides of the flow domain. The atmospheric data used in this study were the daily values of precipitation and potential evapotranspiration measured during the year 1991 in De Bilt, The Netherlands (Figure 3). Bare soil condition was assumed for each simulation and therefore, the potential evapotranspiration values were used as potential evaporation from soil. Simulations were conducted for a sand soil. Since no hydraulic properties have been measured we used the hydraulic properties of the Brooks & Corey model provided by the HYDRUS-2D model.

3. RESULTS AND DISCUSSION

In this section the results of the field experiments and model simulations are presented and discussed. First the soil water content distribution around an AP- and an AT-mine buried in a sand soil is plotted for a period of 6 weeks (January-March 2001). In the same plots also the daily-accumulated precipitation is given. In this way the effect of precipitation and periods of drought on the soil water distribution is seen (§ 3.1.1, § 3.1.2). Next the effect of the mines on the soil water distribution compared to the reference background is given (§ 3.1.3). With an empirical relation between soil water distribution and dielectric constant this effect is translated into a dielectric contrast between mine and soil background (§ 3.1.4). In section 3.1.5 and 3.1.6 effects of soil temperature and WCR on the results is considered. Finally, the simulation results are presented and compared with the field experiments (§ 3.2).

3.1 Measurement of Soil Water Distribution around landmines

3.1.1. Soil water distribution around an AP-mine.

Figure 4 shows the soil water content recordings near an AP-mine in the 'sand' test lane from January 26th – March 9th, 2001. The water content was measured at two depths, 9 cm and 14 cm below surface, just above and just below the AP-mine (respectively sensor 'Sand AP h 46' and 'Sand AP l 45'). Also two reference sensors were installed at the same depths, at 40 cm horizontal distance, respectively sensor 'Sand AP h ref 44' and 'Sand AP l ref 43' (See also Figure 2). From sensor 'Sand AP h 46' only a small set of useful data was available. In the figure also the daily-accumulated precipitation is depicted.

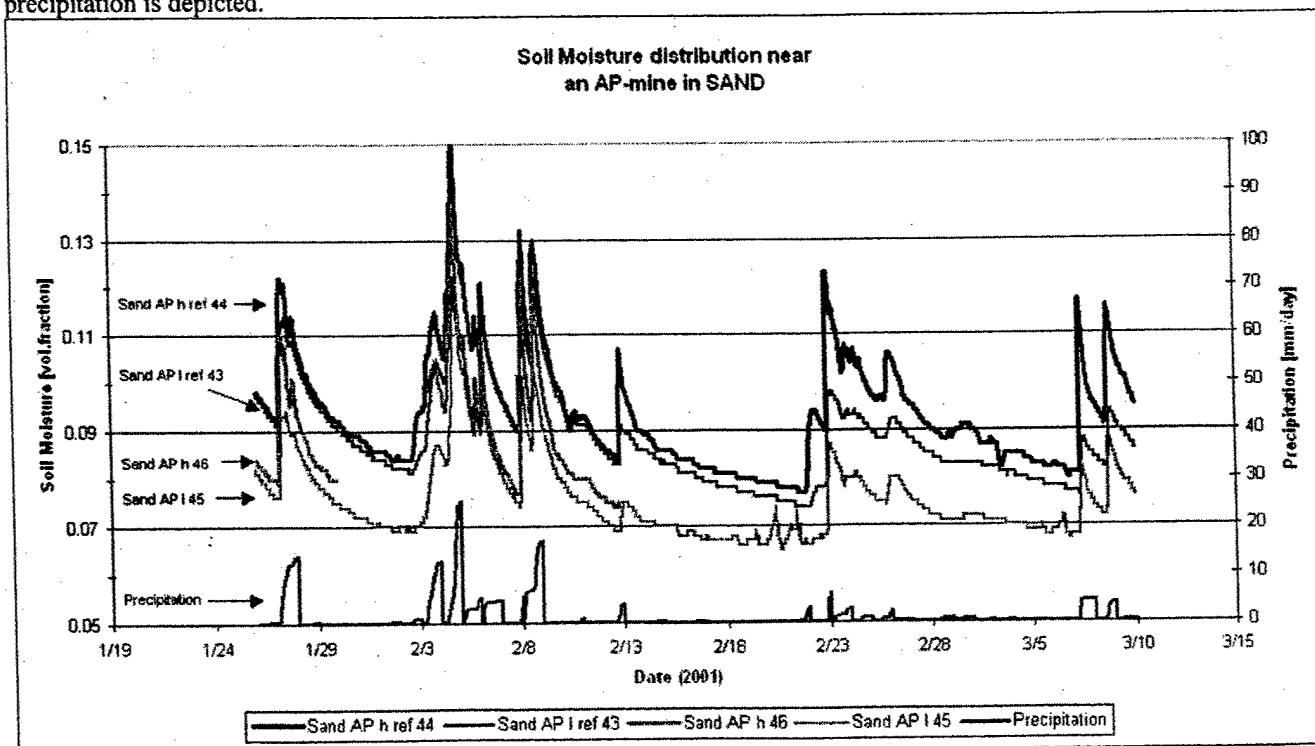


Figure 4. Soil water distribution around an AP-mine in sand.

From Figure 4 it is seen that the soil water content generally increased during a period of precipitation and decreased after a period of drought. The reaction time was generally short (1-2.5 hrs). The water content increased most at shallow depth, and less below the AP-mine. After a period of cumulative 38 mm precipitation (on February 3rd and 4th) water content below the AP-mine increased from 0.07 to 0.12 [m³/m³]. The maximum water content of 0.15 [m³/m³] was measured in the reference background area at a depth of 9 cm.

3.1.2. Soil water distribution around an AT-mine.

Figure 5 shows the soil water content recordings near an AT-mine in the 'sand' test lane from January 26th – March 9th, 2001. The water content was measured at 29 cm and 44 cm depth, just above and just below the AT-mine (respectively sensor 'Sand AT h 54' and 'Sand AT l 53'). Also two reference sensors were installed at the same depths, at 40 cm horizontal distance, respectively sensor 'Sand AT h ref 52' and 'Sand AT l ref 51'. In the figure also the daily-accumulated precipitation is depicted.

From Figure 5 the same general features are noted. The soil water content increased during a period of precipitation and decreased after a period of drought. The reaction time is generally short (3-5 hrs), but twice as long as for the shallower AP sensors. The peaks in the curves are also smoother. After precipitation the water content increased less below than above the AT-mine.

After a period of cumulative 38 mm precipitation (on February 3rd and 4th) water content above the AT-mine increased from 0.09 to 0.17 [m³/m³] and below the mine from 0.09 to 0.13 [m³/m³]. The maximum water content of 0.20 [m³/m³] was measured in the reference background area at a depth of 44 cm.

Around February 23rd the damping effect with depth is clearly visible. The deeper sensors reacted (much) slower on precipitation than the shallow ones. The water content below the AT-mine only increased slowly and only 0.6 %, while the reference area increased faster and more (+1.5 %).

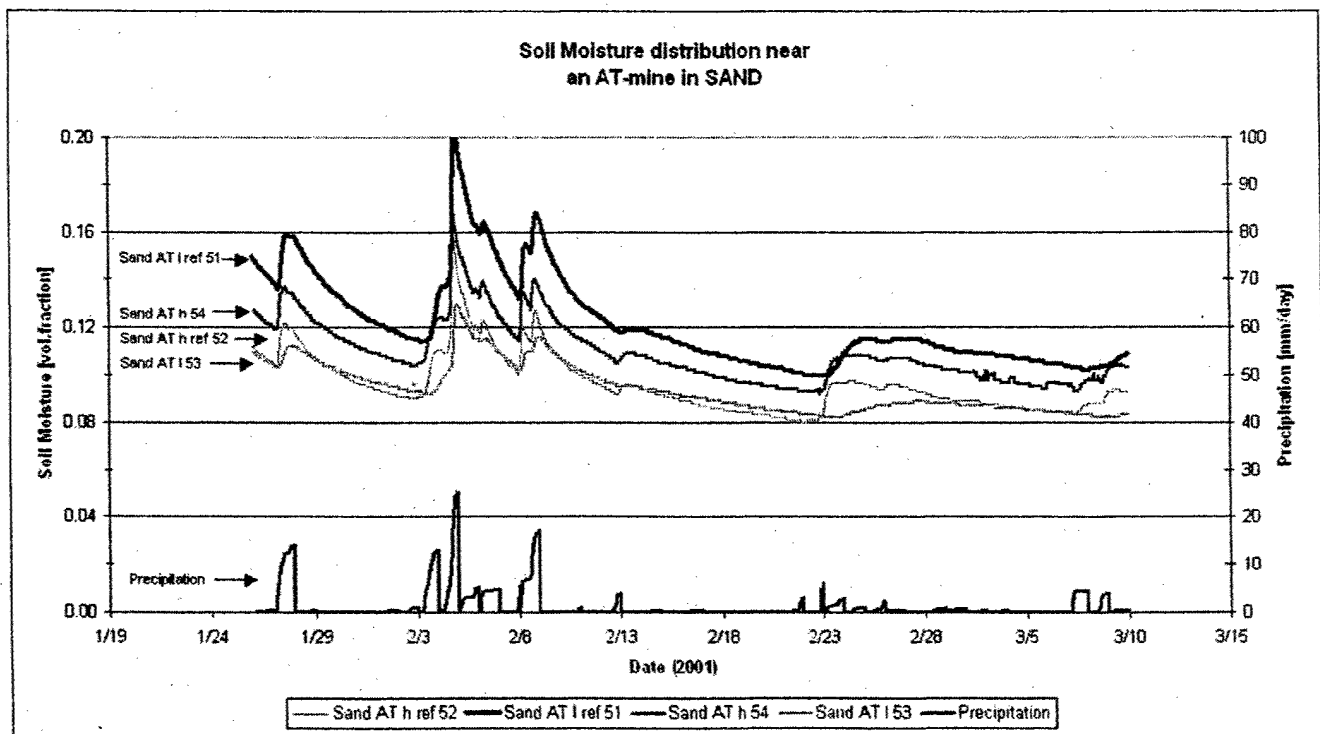


Figure 5. Soil water distribution around an AT-mine in sand.

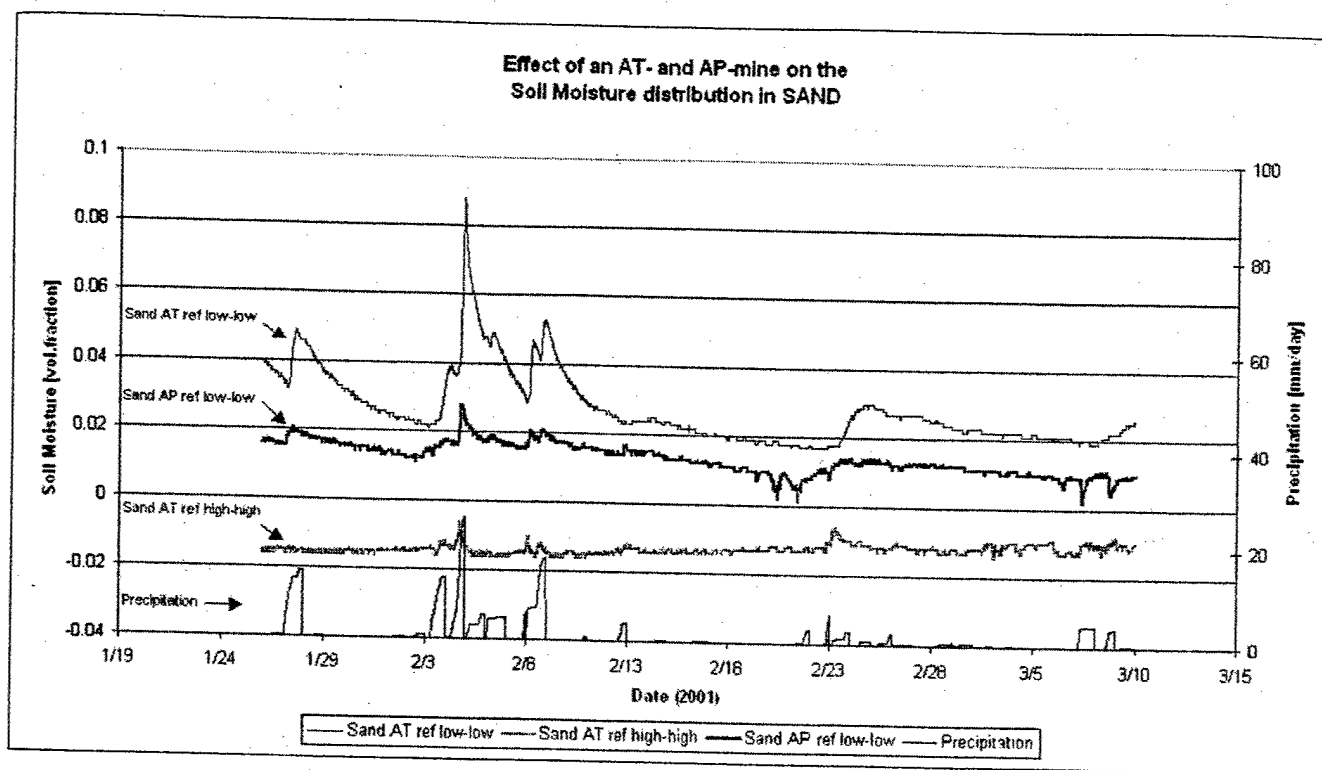


Figure 6. Effect of an AT and AP-mine on the soil water distribution in sand.

3.1.3 Effect AT-and AP-mines of water distribution

In Figure 6 the effect of both the AT- and AP-mine on the soil water distribution in sand is visualized. For the AT-mine the difference in water content above and below the mine with the reference locations is depicted, respectively 'Sand AT ref high-high' and 'Sand AT ref low-low'. For the AP-mine only the difference in soil water content below the mine and the reference is shown ('Sand AP ref low-low'). The set of recordings above the AP-mine was too limited and therefore not shown.

The curve 'Sand AT ref high-high' shows that the difference in soil water content between the soil above the AT-mine and the reference location remained almost constant and thus independent of the amount of precipitation during the trial period. The soil above the AT-mine was always a little (~ 0.01) wetter than the reference location.

The soil below the AT- and AP-mine was always dryer than their reference locations. After a period of precipitation the differences with the reference locations increased ('Sand AT ref low-low' and 'Sand AP ref low-low'). In the dry period these differences decreased. The effect of the AT-mine was larger than the effect of the AP-mine. The difference in soil water content for the AT-mine varied from 0.02 to 0.09 [m^3/m^3] and for the AP-mine from 0.00 to 0.03 [m^3/m^3].

3.1.4. Effect AT-and AP-mines on soil dielectric constant

The dielectric constant (ϵ) is strongly dependent on the volumetric water content (θ_v) of the soil. In addition the dielectric constant was almost independent of soil density, texture and salt content at frequency between 20 MHz and 1 GHz¹¹.

In order to estimate the dielectric constant of the soil around the landmines we will use the calibration curve reported by Topp et al.¹¹:

$$\epsilon = 3.03 + 9.3 \times \theta_v + 146 \times (\theta_v)^2 - 76.7 \times (\theta_v)^3 \quad (\text{Eq. 1})$$

In Figure 7 the results of this calculation are presented for a few situation.

The curve 'AT ref average-TNT' shows the difference in dielectric constant (dielectric contrast) of the reference area at the level of the AT-mine and the mine during the trial. The surrogate and the real AT-mine consist of mainly RTV3110 and TNT, respectively, both with dielectric constants approximately 2.9 [F/m] (Table 1). The dielectric contrast for the reference area and the AT-mine varied from 2.1 [F/m] at the end of a dry period of two weeks (9-23 February) to 6.3 [F/m] after a wet period of cumulative 38 mm precipitation (3-4 February).

Two curves show the dielectric contrast between the soil below the AT- and AP-mine and their reference locations (respectively, and 'Sand AP ref low-low'). The dielectric contrast for the AT-mine ('Sand AT ref low-low') varied from 0.6 [F/m] at the end of the dry period to 4.5 [F/m] after the wet period. The dielectric contrast for the AP-mine ('Sand AP ref low-low') varied from no-contrast at the end of the dry period to 1.3 [F/m] after the wet period.

Two curves show the dielectric contrast between the soil just above and below the AT-mine and the mine. The dielectric contrast between the AT-mine and the sand just above the mine ('Sand AT high-TNT') varied from 2.2 [F/m] at the end of the dry period to 5.4 [F/m] after the wet period. The contrast with the sand just below the AT-mine ('Sand AT low-TNT') varied from 1.8 to 3.6 [F/m], respectively.

Based on these values it can be concluded that during dry periods the contrast between the area with the AT-mine and the background (without mine) is caused by a difference in dielectric constant between the background and the mine. After a dry period of two weeks the contrast with the AT-mine of 2.9 [F/m] was approximately 2 [F/m] higher. After a period of 38 mm precipitation the contrast between AT-mine and background increased to 6.3 [F/m]. The effect of the AT-mine on soil water distribution caused a contrast 4.5 [F/m] between the soil below the mine and the reference area. This effect of the AP-mine was less apparent (1.3 [F/m]).

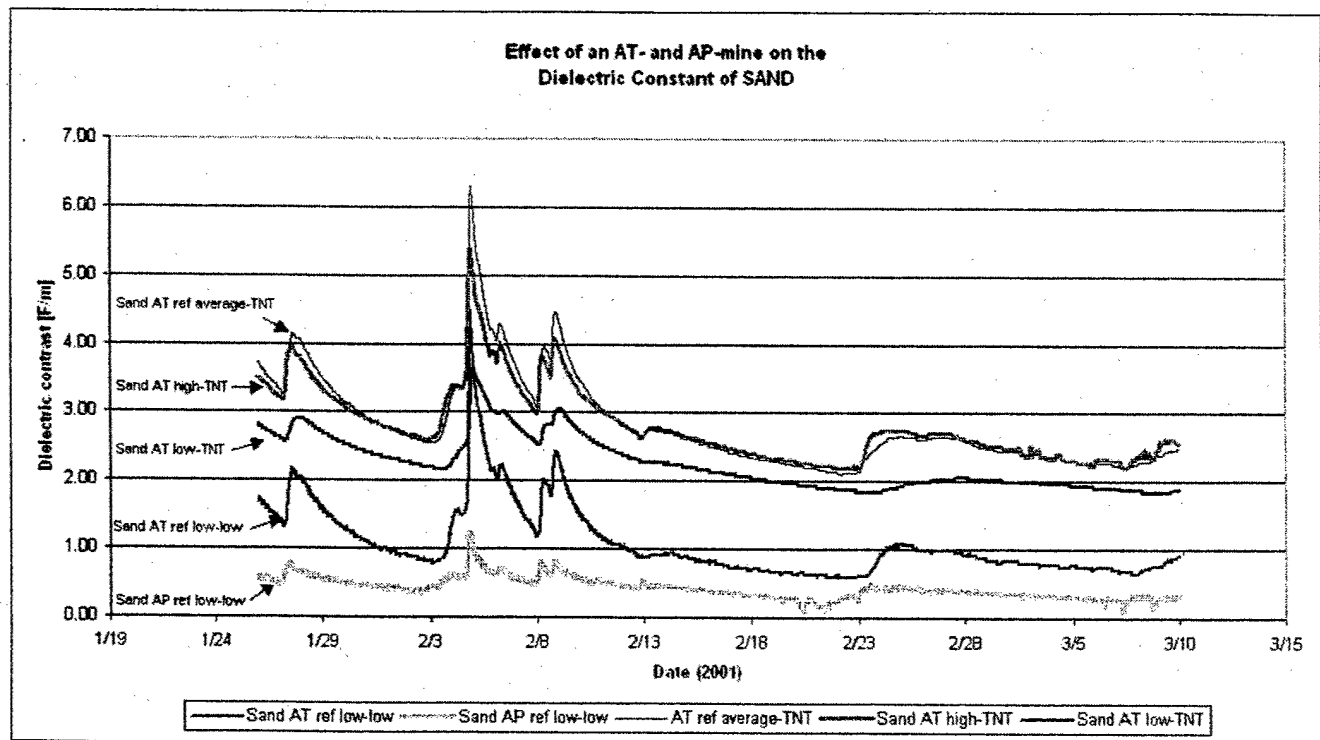


Figure 7. Effect of an AT- and AP-mine on the dielectric constant of sand.

3.1.5. Effect temperature on results.

Figure 8 shows ambient and soil temperature recordings from January 26th – March 9th, 2001. The ambient temperatures were measured at a central location of the test facility at a height of 2 m. The soil temperatures were measured in the 'sand' test lane at a depth of 10 cm and 30 cm.

The average ambient temperature was 4.0°C with a standard deviation of 3.8°C, a maximum of 14.2°C and a minimum of -6.0 °C. The average soil temperature at a depth of 10 cm was 3.6°C with a standard deviation of 2.2°C, a maximum of 8.8°C and a minimum of 0.2°C. The average soil temperature at a depth of 30 cm was 4.1°C with a standard deviation of 1.5°C, a maximum of 7.8°C and a minimum of 1.5°C. Note that the amplitude of the temperature fluctuation decreases with soil depth. Also a phase shift can be noted between ambient temperature and the temperatures at depths of 10 cm and 30 cm.

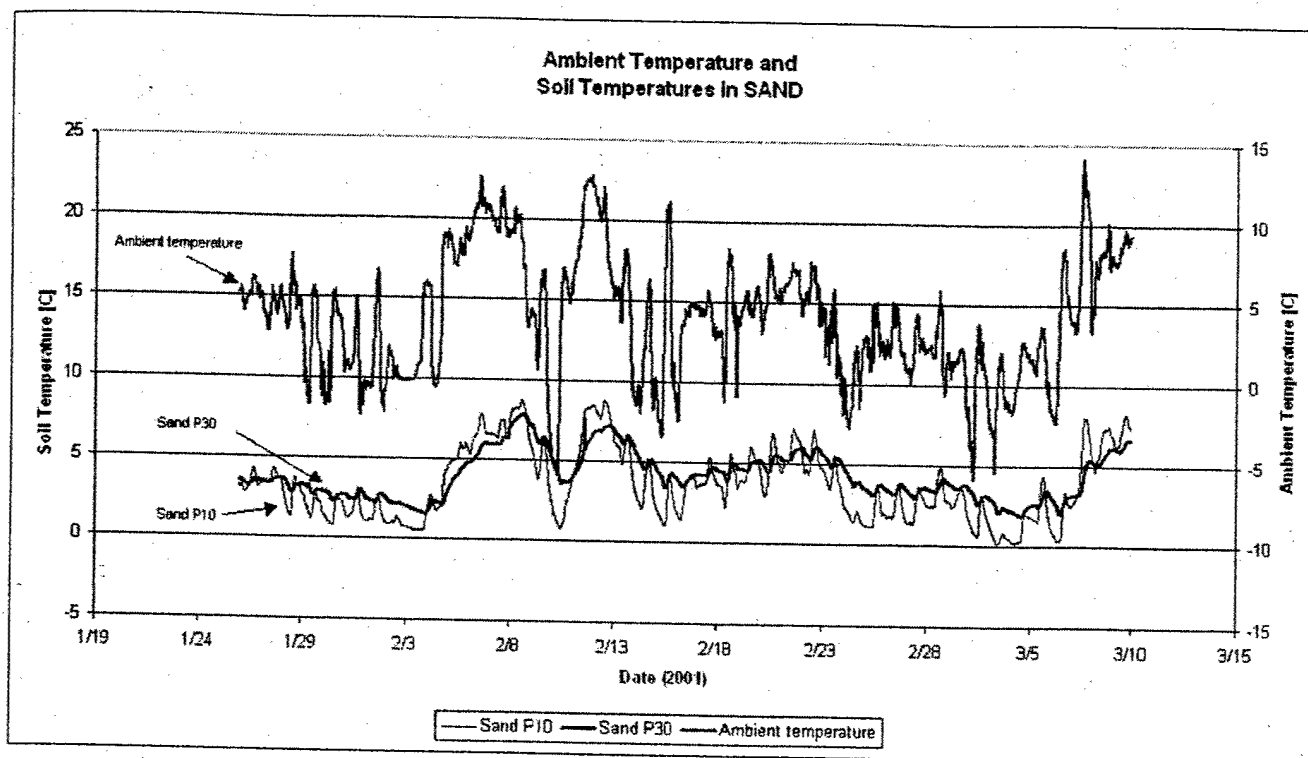


Figure 8. Ambient and soil temperatures in sand test lane (P10, P30 at depth 10 and 30 cm respectively).

The WCR output is sensitive to temperature, and compensation can be applied to enhance accuracy. The magnitude of the temperature coefficient varies with water content. Equation 2 can be used to interpolate the temperature coefficient for a range of volumetric water content (θ_v) values⁴:

$$\text{Coef}_{\text{temperature}} = -3.46 \times 10^{-4} + 0.019 \times \theta_v - 0.045 \times \theta_v^2 \quad [^{\circ}\text{C}^{-1}] \quad (\text{Eq. 2})$$

To apply this correction the following equation can be used (Eq. 3):

$$\theta_{v \text{ corrected}} = \theta_{v \text{ uncorrected}} - (T - 20) \times \text{Coef}_{\text{temperature}} \quad (\text{Eq. 3})$$

T is the soil temperature in $^{\circ}\text{C}$. The uncorrected water content values can be computed from the calibration values mentioned in Table 2. Equation 2 and 3 were determined in the laboratory over a temperature range from 10°C to 30°C .

If this correction is applied for example on the water content measured by the sensor just above the AT-mine ('Sand AT h 54') with the temperatures measured at a depth of 30 cm (Figure 5), the difference between corrected and uncorrected would yield on average 0.02 and maximal 0.03 (volume fraction). For the 'Sand AP 1 45' this correction would yield on average 0.01 with maximum 0.02. Using Equation 1 an average of 0.02 increase in water content for area just above the AT-mine would increase the dielectric constant by approximately 0.8 [F/m]. For the area just below the AP-mine 0.01 increase in soil water content would increase the dielectric constant by 0.3 [F/m]. In both cases the contrast with the mine and therefore the probability of detection increases.

Not using the temperature correction seems acceptable when considering the fact that the possible spatial variation along the 30-cm rods can be of the same order. Moreover equations for the corrections were determined for the temperature range 10 to 30°C . Possibly another correction equation is needed for the lower temperatures.

3.1.6. Effect WCR on results.

The length of the two rods of the WCR is 30 cm. This is equal to the diameter of the AT-mine. However, the diameter of the AP-mine is much smaller: 5.6 cm. The WCR output after calibration gives a water content average for the area close to the

rods. It is therefore possible (and likely) that the soil water values just above and below the AP-mine are differing from the actual values.

The WCR rods were installed at a distance of 1 cm from the top and the bottom of the mines. In free space and dry sand we did not notice any effect of the mine on the recordings. During wet conditions there might be an effect of the mine on the readings. Campbell (oral comm. 2001) reports a penetration depth determined in the laboratory of maximum 2.5 cm from the rod surface. This means that possibly the water content values are underestimated. Due to differences in shape of the top and bottom of the mines, there is also a possibility that this 'blocking' effect is different for both sides of the mines. We did not compensate for these effects.

3.2 Simulation of Soil Water Distribution Around Landmines

Our simulations of soil water content distributions around an anti tank land mine for Dutch weather conditions in a sand soil are very similar to those reported for Sarajevo⁹. Shortly after a precipitation event the soil water content above the mine is larger than below the mine while during dry spells the soil water content above the mine becomes smaller than below the mine (Figure 9).

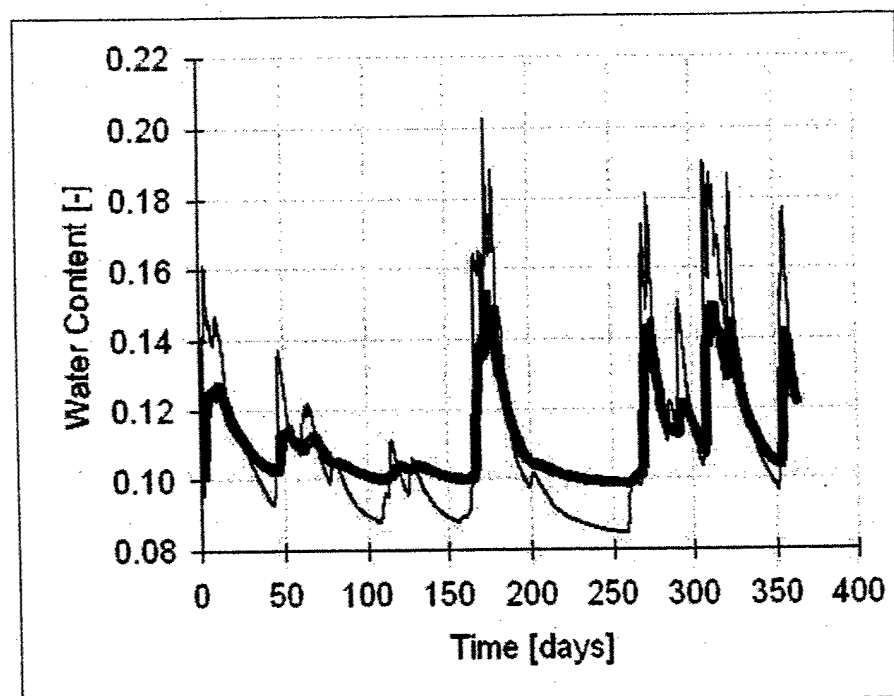


Figure 9. Soil water contents simulated above (thin line) and below (thick line) an AT mine in a sand soil during 1991 at De Bilt, The Netherlands.

4. CONCLUSIONS

The results from the field trial showed a relation between soil water content in a sand soil and precipitation. During a period of precipitation the soil water content near the buried AP- and AT-mines increased. During a period of drought the soil water content decreased. After a period of two days with 38 mm precipitation the water content below the AP-mine increased from 0.07 to 0.12 [m^3/m^3]. The water content above and below the AT-mine increased from 0.09 to 0.17 [m^3/m^3] and 0.09 to 0.13 [m^3/m^3], respectively. Below the AT-mine it was 0.02 to 0.04 [m^3/m^3] dryer than above the mine.

The differences in water content between the soil just below the AP-mine and the reference background soil (at the same depth) varied during the field trial from 0.00 to 0.03 [m^3/m^3]. The differences in water content between the soil just above and below the AT-mine and their respective reference backgrounds varied from 0.01 to 0.02 [m^3/m^3] and 0.02 to 0.09 [m^3/m^3], respectively. Below the both mines it was always dryer than the reference background. Above the AT-mine it was always dryer than the background. The low contrast values occurred during dry periods. The high contrast values occurred during periods of precipitation.

The dielectric contrast between the buried landmines and the background soil was estimated using an empirical relation between soil water content and dielectric constant. During dry periods the contrast between the area with the AT-mine and

the reference background is caused by a difference in dielectric constant between the background and the mine. After a dry period of two weeks the contrast with the AT-mine (with dielectric constant of 2.9 [F/m]) was approximately 2 [F/m]. After a period of 38 mm precipitation the contrast between AT-mine and background increased to 6 [F/m].

The effect of the AT-mine on soil water distribution caused a maximum contrast 4.5 [F/m] between the soil below the mine and the reference area. This effect of the AP-mine was less apparent, 1.3 [F/m].

In the presence of a buried landmine in the sand soil caused a dielectric contrast with the background soil. This contrast increased when the soil water content increased as a result of precipitation, and decreased as a result of drought. It is therefore likely that also the probability of detection of the landmines with a GPR increases with an increase of soil water content, and decreases with a decrease of soil water content.

The model simulations of soil water content distributions around the AT-mine for Dutch weather conditions (of 1991) in a sand soil showed an increase in soil water content above and below the mine shortly after a precipitation event. The soil water content above the mine was larger than below the mine while during dry spells the soil water content above the mine became smaller than below the mine. During the field trial below the AT-mine it was always 0.02 to 0.04 [m^3/m^3] dryer than above the mine. Further investigation is needed to explain this difference.

ACKNOWLEDGEMENTS

The TNO-FEL contribution to this work was sponsored by the HOM-2000 project. The U.S. Army Research Office (ARO) sponsored the NMT contribution. Further do we acknowledge useful inputs from Dr. Russell Harmon (ARO) and Peter Fritz (TNO-FEL).

REFERENCES

1. Borchers B., Hendrickx J.M.H., Das B.S. and S. Hong. *Enhancing dielectric contrast between land mines and the soil environment by watering: modeling, design, and experimental results*. In 'Detection and Remediation Technologies for Mines and Minelike Targets V', Proceedings SPIE-Orlando Vol. 4038 pp 993-1000, April 2000.
2. De Amici G. and B. Hauss. *Cryogenics as a means to improve the detection of landmines*. In 'Detection and Remediation Technologies for Mines and Minelike Targets V', Proceedings SPIE-Orlando Vol. 4038 pp 270-276, April 2000.
3. W. de Jong, H.A. Lensen, Y.H.L. Janssen, *Sophisticated test facility to detect land mines*. In 'Detection and Remediation Technologies for Mines and Minelike Targets IV', Proceedings SPIE-Orlando Vol. 3710 pp 1409-1418, April 1999.
4. *CS615 Water Content Reflectometer instruction manual*, version 8221-07, revision 10/96. Campbell Scientific, Inc., Logan, Utah 84321-1784, 1996.
5. *Product Information for Silastic 3110 RTV Silicone Rubber*. Dow Corning Europe, Brussels, 1981, Data Sheet number 61-143-01.
6. Patel D.L. *Handbook of Land Mines and Military Explosives for Countermine Exploitation*. US Army, Belvoir Research, Development and Engineering Center, Fort Belvoir, Virginia, 1992, US Army report, 2495.
7. Dobratz B.M. and P.C. Crawford, *LLNL Explosives Handbook; Properties of Chemical Explosives and Explosive Simulant*. Lawrence Livermore National Laboratory; University of California, Livermore, California, 1985, UCRL-52997.
8. Šimunek, J., Šejna M. and M. Th. Van Genuchten. *HYDRUS-2D/MESHGEN-2D code for simulating water flow and solute transport in two-dimensional variably saturated media*. IGWMC - TPS 53C, Ver. 2.01, International Ground Water Modeling Center, Colorado School of Mines, CO 80401, USA. 1999.
9. Das, B.S., Hendrickx J.M.H. and B. Borchers. *Modeling transient water distributions around landmines in bare soils*. Soil Science vol. 166, in press.
10. Hendrickx, J.M.H., B.S. Das, and B. Borchers. *Modeling distributions of water and dielectric constants around landmines in homogeneous soils*. Proceedings SPIE Vol. 3710, Detection and Remediation Technologies for Mines and Minelike Targets IV, p. 728-738. 1999.
11. Topp G.C., Davis J.L. and A.P. Annan. *Electromagnetic Determination of Soil Water Content: Measurements in Coaxial Transmission Lines*. Water Resources Research, vol. 16, no.3, pp 574-582, June 1980.